

# Large Non-Gaussianities in Single Field Inflation

Xingang Chen<sup>1</sup>, Richard Easther<sup>2</sup> and Eugene A. Lim<sup>2</sup>

<sup>1</sup> Newman Laboratory, Cornell University, Ithaca, NY 14853

<sup>2</sup> Department of Physics, Yale University, New Haven, CT 06511

## Abstract

We compute the 3-point correlation function for a general model of inflation driven by a single, minimally coupled scalar field. Our approach is based on the numerical evaluation of both the perturbation equations and the integrals which contribute to the 3-point function. Consequently, we can analyze models where the potential has a “feature”, in the vicinity of which the slow roll parameters may take on large, transient values. This introduces both scale and shape dependent non-Gaussianities into the primordial perturbations. As an example of our methodology, we examine the “step” potentials which have been invoked to improve the fit to the glitch in the  $\langle TT \rangle C_\ell$  for  $\ell \sim 30$ , present in both the one and three year WMAP data sets. We show that for the typical parameter values, the non-Gaussianities associated with the step are far larger than those in standard slow roll inflation, and may even be within reach of a next generation CMB experiment such as Planck. More generally, we use this example to explain that while adding features to potential can improve the fit to the 2-point function, these are *generically* associated with a greatly enhanced signal at the 3-point level. Moreover, this 3-point signal will have a very nontrivial shape and scale dependence, which is correlated with the form of the 2-point function, and may thus lead to a consistency check on the models of inflation with non-smooth potentials.

# 1 Introduction

The Cosmic Microwave Background is a treasure trove of information about the primordial universe. An exciting set of current and future experiments [1, 2, 3] will yield an even richer data set, information that will allow us to make precise tests of inflationary models via their predictions for the form of the primordial perturbations. Typically, these predictions are expressed in terms of the power spectrum, or 2-point function. For a general set of initial inhomogeneities, we might expect that further information about the perturbations could be gleaned from their higher order correlation functions. If the perturbations are exactly Gaussian, then the  $N$ -point functions would vanish exactly when  $N$  is odd, and would be fully specified in terms of the 2-point function for even  $N$ .

All inflationary models predict *some* level of non-Gaussianity, which manifests itself via  $N$ -point functions which differ from those expected for strictly Gaussian perturbations. Moreover, non-linear corrections will generate non-Gaussianities in the CMB even if the primordial spectrum is purely Gaussian [4]. Thus any observed non-Gaussianities will be a combination of both the primordial non-Gaussianity, which is laid down during inflation, and those that arise due to weak nonlinear coupling between modes which arise at second order in gravitational perturbation theory. A rough measure of the non-Gaussianities is provided by the parameter  $f_{NL}$ ,

$$\Phi(x) = \Phi_L(x) + f_{NL}(\Phi_L(x)^2 - \langle \Phi_L(x)^2 \rangle) \quad (1.1)$$

where  $\Phi(x)$  is the gravitational potential which sources the temperature anisotropies in the CMB [5]. Generically, second order couplings between modes yields  $f_{NL} \approx O(1)$ , while it has been shown in great detail that for standard single field slow roll inflation,  $f_{NL} \sim \epsilon \sim O(10^{-2})$ , where  $\epsilon$  is the usual slow roll parameter [6]. The two contributions are cumulative, and the primordial 3-point function is thus swamped by the evolutionary contribution. Moreover, cosmic variance ensures that even a perfect CMB dataset will not provide a conclusive detection of the 3-point function if  $f_{NL}$  is of order unity. In addition, the presence of foreground contamination [2, 7] further complicates observational efforts. Current estimates suggest that Planck can achieve a limit of  $|f_{NL}| < 20 \sim 30$  [8]. As we will show in this paper, this may be sufficiently sensitive to permit the detection of interesting features in the 3-point statistics for some classes of scale-dependent inflationary models.

The 3-point correlation function is a separate and independent statistic. Therefore it potentially provides a method for discriminating between models of inflation with degenerate power spectra. More optimistically, if the amplitude of the 3-point function is large enough for us to *map* its dependence on both the *scale* and *shape* of the momenta triangle, this will be an enormous boon to early universe cosmology, since the 3-point function encodes information in both these properties. However, to be able to realize this possibility, we need to be able to both predict the 3-point correlation function given an inflationary model, and compare these predictions to data. Our goal here is to show how to compute the 3-point function for a general model of inflation driven by a single, minimally coupled scalar field. Crucially, we do not assume slow roll, and our methodology thus applies to both simple models with smooth potentials, and also more complicated scenarios where the potential has an isolated “feature”. Since the 3-point function can have both shape and scale dependence,

our calculations will underscore the limitations of a single scalar statistic such as  $f_{NL}$ . Our analysis is purely theoretical, and we do not directly consider the problem of performing a comparison between our computed 3-point function and data, but this issue is being actively addressed by others [9].

Our interest in this problem is motivated by the observation that as cosmological data improves, we will frequently be faced with the problem of interpreting “glitches” in the observed power spectra, and determining whether these represent genuine departures from some concordance cosmology. For instance, the  $C_\ell$  derived from the temperature anisotropies in both the 1 Year and 3 Year WMAP datasets show a noticeable departure from the best fit LCDM spectra around  $\ell \sim 30$ , and the fit can be improved by adding a small “step” to the inflationary potential. The best-fit parameters for this step were extracted from the 1 Year data set in [10], and from the 3 Year dataset in [11], and the two analyses find broadly similar values. Of course, any proposal that adds free parameters to the inflationary potential is likely to produce a better fit to data. The question then turns to whether this improvement is good enough to justify the additional parameters. If we focus solely on the 2-point function, this question is addressed via the resulting change in the  $\chi^2$  per degree of freedom, or by Bayesian evidence. However, we will see that a potential with a sharp, localized feature induces a massive enhancement of the primordial 3-point function, relative to our expectations from slow-roll. In particular, this enhancement is sufficiently dramatic to boost the non-Gaussianities to the point where it is reasonable to hope they can be detected experimentally. Consequently, this provides a stringent check on any proposal for a nontrivial inflationary potential, since the specific form of the non-Gaussianities will be heavily correlated with the 2-point function. Such correlations will extend to higher order statistics such as the trispectrum and beyond, though we do not consider them here [12, 13, 14, 15, 16, 17, 18].

In this paper we show how to compute the 3-point function for an arbitrary inflationary model driven by a single, minimally coupled scalar field. This necessitates a numerical treatment, but we begin by showing that we can recover existing semi-analytical results that assume slow roll. A similar analytical estimate was also done in [19] which broadly collaborates with what we calculated here. We then analyze a specific model where the inflaton potential has a small, sharp “step” [20] to illustrate our methodology in a non-trivial setting. In particular, since this model has already been used to improve the fit between LCDM cosmology and the observed power spectrum, we can take the resulting best-fit parameter values for this step and compute the resulting 3-point function. Interestingly, although such a feature only causes a small correction in the 2-point correlation function (which was used to simulate the glitch in the CMB power spectrum), it amplifies the non-Gaussianity by a factor of order 1000. Roughly speaking<sup>1</sup>, the estimator  $f_{NL}$  is boosted from  $\mathcal{O}(.01)$  to  $\mathcal{O}(10)$ . This makes the non-Gaussianity a potentially useful constraint on such models. In particular, the leading term in the cubic Lagrangian that is responsible for this boost is different from those used in the previous calculations in Ref. [6, 21, 22].

The most distinctive feature of this non-Gaussianity is its characteristic running, defined as its dependence on the scale of the momenta triangle [23]. Firstly, this large non-

---

<sup>1</sup>As we will discuss later,  $f_{NL}$  is not a good statistic for such non-trivial non-Gaussianities, but it is a good estimate.

Gaussianity has a very characteristic “ringing” behavior; as we will see, a suitably defined estimator roughly similar to  $f_{NL}$  oscillates between positive and negative values. Secondly, the impact on the 3-point function is localized around the wavenumbers that are most affected by any feature, and dies away over a couple of e-folds. These features make it very distinguishable from other single field theories with large non-Gaussianities, such as the DBI inflation [24, 25] or k-inflation models [26], where the non-Gaussianities are present at all scales and the running is very slow [27, 23, 22, 28, 29].

This paper is divided in the following sections. Section 2 details the step potential model that we are considering; we lay out our conventions in this section. Section 3 details the analytic forms of the 3-pt correlation functions, which we will proceed to integrate numerically in Section 4. We discuss our results in Section 5 and conclude in Section 6.

## 2 Slow roll model with a feature

For single field inflation driven by a minimally coupled scalar, the action is

$$S = \int dx^4 \sqrt{g} \left[ \frac{M_p^2}{2} R + \frac{1}{2} (\partial\phi)^2 - V(\phi) \right] \quad (2.2)$$

where the potential  $V(\phi)$  is designed such that the inflaton field  $\phi$  is slowly rolling for long enough to drive inflation. We define the slow roll parameters by<sup>2</sup>

$$\epsilon = \frac{\dot{\phi}^2}{2M_p^2 H^2}, \quad (2.3)$$

$$\eta = \frac{\ddot{\phi}}{\epsilon H}. \quad (2.4)$$

In a plain vanilla slow roll model, say the quadratic chaotic model of  $V(\phi) = (1/2)m^2\phi^2$ , then  $\eta = 2\epsilon$ . Assuming transplanckian field values of  $\phi > M_p$ , both slow roll parameters and their higher derivative cousins are sub-unity.

In this paper we add a step into the slow roll potential in the form proposed by [20]

$$V(\phi) = \frac{1}{2} m^2 \phi^2 \left[ 1 + c \tanh \left( \frac{\phi - \phi_s}{d} \right) \right], \quad (2.5)$$

where the potential has a step at  $\phi_s$ , with size  $c$  and gradient  $d$  respectively. While the presence of the step at just the “right” place would require a tuning, one can imagine potentials with many steps, so that the odds are high that at least one of them would fall inside the range of  $\phi$  relevant to the cosmological perturbations.

As discussed in [31, 20] the presence of this step induces an oscillatory ringing in the power spectrum. When the inflaton rolls down this steep step, it undergoes a strong momentary acceleration, thus violating slow roll. In realistic models the step is typically less than 1% of the overall height of the potential. In this case,  $\dot{\phi}^2 \ll V(\phi)$  at all times, and  $\epsilon \ll 1$ . On the

---

<sup>2</sup>Note these are related to the potential slow roll parameters via  $\epsilon_V = (M_p^2/2)(V'/V)^2$ ,  $\eta_V = M_p^2 V''/V$ , by  $\epsilon = \epsilon_V$ ,  $\eta = -2\eta_V + 4\epsilon_V$ .

other hand,  $\eta \propto V''$  and its higher derivatives can grow dramatically as the inflaton crosses the step, often to the point where they exceed unity, as shown in Fig. (1).

Beyond linear gravity, the modes are coupled through terms proportional to the quadratic and higher products of the slow roll parameters; these ultimately source the non-Gaussianities that we see in the sky. In the following we give an order of magnitude estimate of the values of the slow roll parameters to better understand some of the qualitative behavior. We will see later that the pertinent term that leads to a large boost in non-Gaussianity is proportional to  $\dot{\eta}$  so we will focus on its value here. The step in the potential (2.5) has a depth  $\Delta V \approx (1/2)cm^2\phi^2$  and a width  $\Delta\phi \approx d$  (setting  $M_p = 1$ ). When the inflaton falls down the step,  $\Delta V$  of the potential energy is converted to kinetic energy, resulting in an increase in  $\epsilon$  on the order of  $\Delta\epsilon \approx \Delta V/H^2 \approx 3c$ , within a time interval  $\Delta t \approx \Delta\phi/\dot{\phi} \approx d/\sqrt{2cV}$ . Using these quantities, we can estimate

$$\eta = \frac{\dot{\epsilon}}{H\epsilon} \approx \frac{3\sqrt{6} c^{3/2}}{d\epsilon} \quad (2.6)$$

and

$$\begin{aligned} \dot{\eta} &= H\left(\frac{\ddot{\epsilon}}{H^2\epsilon} + \epsilon\eta - \eta^2\right) \\ &\approx H\frac{18c^2}{d^2\epsilon} \left(1 + \frac{d\epsilon}{\sqrt{6}c} - \frac{3c}{\epsilon}\right) \\ &\approx H\frac{18c^2}{d^2\epsilon}. \end{aligned} \quad (2.7)$$

These values correspond to the order of magnitude of the peaks in the numerical solutions in Fig. 1.

After this acceleration, the inflaton is damped by the friction term in the equation of motion

$$\ddot{\phi} + 3H\dot{\phi} + \frac{dV}{d\phi} = 0 \quad (2.8)$$

and relaxes to the attractor solution. This relaxation time is determined by the first two terms in Eq. (2.8), and the order of magnitude is  $H^{-1}$ . This time duration corresponds to the *decay* width of the peaks in Fig. 1. Our numerical results were computed with  $c = 0.0018$ ,  $d = 0.022$  – the central values of the step corresponding to the low- $\ell$  glitch analyzed by Covi *et al.* [11]. Thus  $\epsilon \approx 2/\phi^2 \approx 2/14.8^2$ , and get  $\eta' \approx 18c^2/(d^2\epsilon) \approx 13$  ( $aH \approx -1/\tau$  is chosen to be around 1 in the plot, and  $\tau$  is the conformal time), consistent with Fig. 1. As we will see later, the leading term in the 3-point expansion for this model is proportional to  $\eta'\epsilon$  which will be of  $\mathcal{O}(1000)$  times the  $\epsilon^2$  terms. We will see later that such a feature persists for around one e-fold of inflation.

Since the non-linear couplings of the perturbations are proportional to powers of the slow roll parameters which characterize the background evolution – even in the non-slow roll regime – a deviation from slow roll results in a large mixing (“interaction”) of modes generating large non-Gaussianities. In the next section, we will lay out the formalism for the calculation of this non-Gaussianity.

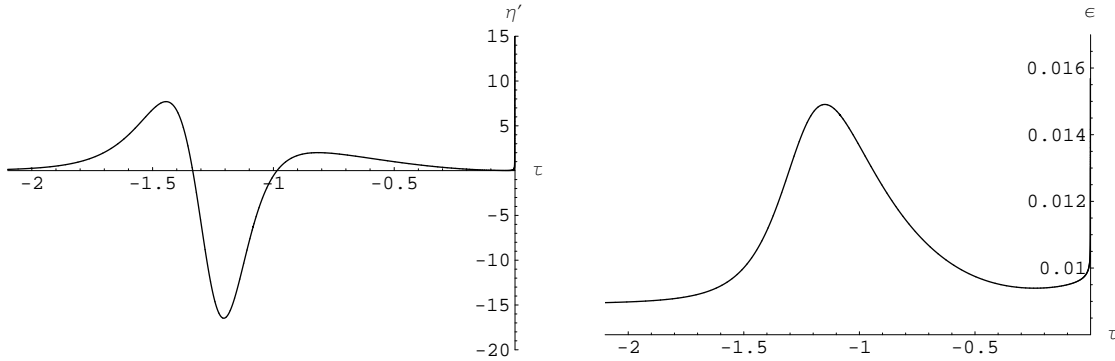


Figure 1: The  $\eta'$  (left) and  $\epsilon$  (right) evolution over the step for the model  $c = 0.0018$ ,  $d = 0.022$ , with its amplitude momentarily  $\eta' \approx 18c^2/(\epsilon d^2)$ . This turns out to be the primary source of the large non-Gaussianities in the step potential model as the leading term in the 3 point expansion is of order  $\eta'\epsilon$ . On the other hand, since the step is very shallow (though it is steep), the ratio of the kinetic energy to the potential energy remains tiny and thus  $\epsilon$  remains sub-unity.

### 3 3-point correlation functions

In this section, we sketch out the derivation of the 3-point correlation function, following [6, 21, 22]. Our goal is to write down the function as a integral over conformal time  $\tau$ , with the integrand being a finite expansion in slow roll parameters. Although we work with the step potential, the analysis is applicable to any generic sharp feature we might add to the potential.

We begin by perturbing the fields in the ADM metric [32]

$$ds^2 = -N^2 dt^2 + h_{ij}(dx^i + N^i dt)(dx^j + N^j dt) \quad (3.9)$$

using the comoving gauge [33, 6]

$$h_{ij} = a^2 e^{2\zeta} \delta_{ij} \ , \quad (3.10)$$

where  $N$  and  $N^i$  are Lagrangian multipliers, and  $\zeta$  is the scalar perturbation. Note that in this gauge  $\delta\phi$  vanishes.

The power spectrum is given by the 2-point correlation function of the curvature perturbation

$$\begin{aligned} \langle \zeta(\mathbf{x})\zeta(\mathbf{x}) \rangle &= \int \frac{d^3 k_1}{(2\pi)^3} \frac{d^3 k_2}{(2\pi)^3} \langle \zeta(\mathbf{k}_1)\zeta(\mathbf{k}_2) \rangle e^{i(\mathbf{k}_1+\mathbf{k}_2)\cdot\mathbf{x}} \\ &= \int \frac{dk}{k} P_\zeta \ , \end{aligned} \quad (3.11)$$

where  $P_\zeta$  is the power spectrum.

The 3-point correlation function is substantially more complicated than its 2-point counterpart. As non-Gaussianities arise from departures from linear order in the equations of

motion, we must compute the action (2.2) to cubic order in the perturbation:

$$\begin{aligned}
S_3 &= \int dt d^3x \{ a^3 \epsilon^2 \zeta \dot{\zeta}^2 + a \epsilon^2 \zeta (\partial \zeta)^2 - 2a \epsilon \dot{\zeta} (\partial \zeta) (\partial \chi) \\
&+ \frac{a^3 \epsilon}{2} \frac{d\eta}{dt} \zeta^2 \dot{\zeta} + \frac{\epsilon}{2a} (\partial \zeta) (\partial \chi) \partial^2 \chi + \frac{\epsilon}{4a} (\partial^2 \zeta) (\partial \chi)^2 + 2f(\zeta) \frac{\delta L}{\delta \zeta} |_1 \} , \quad (3.12)
\end{aligned}$$

where

$$\chi = a^2 \epsilon \partial^{-2} \dot{\zeta} , \quad (3.13)$$

$$\frac{\delta L}{\delta \zeta} |_1 = a \left( \frac{d\partial^2 \chi}{dt} + H \partial^2 \chi - \epsilon \partial^2 \dot{\zeta} \right) , \quad (3.14)$$

$$f(\zeta) = \frac{\eta}{4} \zeta^2 + \text{terms with derivatives on } \zeta . \quad (3.15)$$

Here  $\partial^{-2}$  is the inverse Laplacian and  $\delta L / \delta \zeta |_1$  is the variation of the quadratic action with respect to the perturbation  $\zeta$ . The cubic action (3.12) is exact for arbitrary  $\epsilon$  and  $\eta$ . Note that the highest power of slow-roll parameters which appears is of  $\mathcal{O}(\epsilon^3)$ , when we recall that  $\chi$  contains a multiplicative factor of  $\epsilon$ . The fact that the series expansion in slow-roll parameters is finite is important since, although  $\epsilon$  remains small in the presence of a feature,  $\eta$  and  $\eta'$  may become large. The last term in the action (3.12) can be absorbed by a field redefinition of  $\zeta$ ,

$$\zeta \rightarrow \zeta_n + f(\zeta_n) . \quad (3.16)$$

After this redefinition, the interaction Hamiltonian in conformal time is

$$\begin{aligned}
H_{int}(\tau) &= - \int d^3x \left\{ a \epsilon^2 \zeta \zeta'^2 + a \epsilon^2 \zeta (\partial \zeta)^2 - 2 \epsilon \zeta' (\partial \zeta) (\partial \chi) \right. \\
&\left. + \frac{a}{2} \epsilon \eta' \zeta^2 \zeta' + \frac{\epsilon}{2a} (\partial \zeta) (\partial \chi) (\partial^2 \chi) + \frac{\epsilon}{4a} (\partial^2 \zeta) (\partial \chi)^2 \right\} . \quad (3.17)
\end{aligned}$$

It is more convenient to work in Fourier space, so

$$\langle \zeta(\mathbf{x}) \zeta(\mathbf{x}) \zeta(\mathbf{x}) \rangle = \int \frac{d^3 k_1}{(2\pi)^3} \frac{d^3 k_2}{(2\pi)^3} \frac{d^3 k_3}{(2\pi)^3} \langle \zeta(\mathbf{k}_1) \zeta(\mathbf{k}_2) \zeta(\mathbf{k}_3) \rangle e^{i(\mathbf{k}_1 + \mathbf{k}_2 + \mathbf{k}_3) \cdot \mathbf{x}} . \quad (3.18)$$

The field redefinition equation (3.16) introduces some extra terms in the 3-point correlation function,

$$\begin{aligned}
\langle \zeta(\mathbf{k}_1) \zeta(\mathbf{k}_2) \zeta(\mathbf{k}_3) \rangle &= \langle \zeta_n(\mathbf{k}_1) \zeta_n(\mathbf{k}_2) \zeta_n(\mathbf{k}_3) \rangle \\
&+ \eta \langle \zeta_n^2(\mathbf{k}_1) \zeta_n(\mathbf{k}_2) \zeta_n(\mathbf{k}_3) \rangle + \text{sym} + \mathcal{O}(\eta^2 (P_k^\zeta)^3) , \quad (3.19)
\end{aligned}$$

where  $\zeta_n^2(\mathbf{k})$  denotes the Fourier transform of  $\zeta_n^2(\mathbf{x})$  – we stress that this is not the square of  $\zeta_n(\mathbf{k})$ . In (3.19), the slow roll parameters are evaluated at the end of inflation. Although we can no longer perturbatively expand in terms of  $\eta$  if  $\eta$  is large, the terms that we neglected are of higher order in  $P_k^\zeta$ . Since  $P_k^\zeta \sim 10^{-10}$ , we can neglect these unless  $\eta$  is ridiculously

large – which it never does in any case of interest to us. In addition, we have only considered the first term in (3.15), since all other terms involve at least one derivative of  $\zeta$ , and vanish when evaluated outside the horizon.

The 3-point correlation function at some time  $\tau$  after horizon exit is then the vacuum expectation value of the three point function in the interaction vacuum

$$\langle \zeta(\tau, \mathbf{k}_1) \zeta(\tau, \mathbf{k}_2) \zeta(\tau, \mathbf{k}_3) \rangle = -i \int_{\tau_0}^{\tau} d\tau' a \langle [\zeta(\tau, \mathbf{k}_1) \zeta(\tau, \mathbf{k}_2) \zeta(\tau, \mathbf{k}_3), H_{int}(\tau')] \rangle . \quad (3.20)$$

Before we proceed, let us pause and point out a subtlety hidden inside equation (3.20): the 3-point on the left hand side is evaluated with the *interaction* vacuum while the the right hand side is evaluated at the “true” vacuum. The interaction Hamiltonian  $H_{int}$  evolves the true vacuum to the interaction vacuum at the time we evaluate the 3-point function. Neglecting this will lead to errors as first pointed out by Maldacena [6, 34, 35].

Note that the three terms in the second line of (3.17), which are of higher order in slow-roll parameters, were properly neglected in Refs. [6, 21, 22]. These papers all assume that  $\eta$  and  $\epsilon$  are always small when evaluating the 3-point function, and these terms are thus sub-leading. In this paper, the  $\epsilon^3$  terms are still small, but the  $\epsilon\eta'$  term may be large for the potentials discussed here. In fact, this term will dominate the other terms when slow roll is violated at the step.

We now decompose  $\zeta$  into its Fourier modes and quantize it by writing

$$\zeta(\tau, \mathbf{x}) = \int \frac{d^3\mathbf{P}}{(2\pi)^3} \zeta(\tau, \mathbf{k}) e^{i\mathbf{P}\cdot\mathbf{x}} , \quad (3.21)$$

with associated operators and mode functions

$$\zeta(\tau, \mathbf{k}) = u(\tau, \mathbf{k}) a(\mathbf{k}) + u^*(\tau, -\mathbf{k}) a^\dagger(-\mathbf{k}) , \quad (3.22)$$

where  $a$  and  $a^\dagger$  satisfy the commutation relation  $[a(\mathbf{k}), a^\dagger(\mathbf{k}')] = (2\pi)^3 \delta^3(\mathbf{k} - \mathbf{k}')$ . The “true” vacuum is the one annihilated by the lowering operator  $a(\mathbf{k})$ . The power spectrum is then

$$P_\zeta \equiv \frac{k^3}{2\pi^2} |u_{\mathbf{k}}|^2 . \quad (3.23)$$

with  $u_{\mathbf{k}}$  is  $u(\tau, \mathbf{k})$  evaluated after each mode crosses the horizon.

Meanwhile  $v(\tau, \mathbf{k})$  is the solution of the linear equation of motion of the quadratic action,

$$v_k'' + k^2 v_k - \frac{z''}{z} v_k = 0 , \quad (3.24)$$

where we have used the definitions

$$v_k \equiv z u_k , \quad z \equiv a\sqrt{2\epsilon} . \quad (3.25)$$

Our choice of vacuum implies that the initial condition for the mode function is given by the Bunch-Davies vacuum

$$\begin{aligned} v_k(\tau_0) &= \sqrt{\frac{1}{2k}} \\ v_k'(\tau_0) &= -i\sqrt{\frac{k}{2}} \end{aligned} \quad (3.26)$$

where we have neglected an irrelevant phase, since (3.24) is rotationally invariant.

To compute the 3-point correlation function, one simply substitutes these solutions into equation (3.17), and integrates the mode functions from  $\tau_0$  through to the end of inflation. This integral can be done semi-analytically for simple models, provided the slow roll parameters are small and relatively constant. Any departures from this serene picture will generally make the semi-analytic approach intractable – including the step potential we consider here.

Inspecting equations (3.17) and (3.20) and recalling that  $\chi_k \propto \epsilon \dot{\zeta}_k$ , it is clear that the 3-point correlation function consists of a sum of integrals of the form

$$I_{\epsilon^2} \propto \Re \left[ \prod_i u_i(\tau_{end}) \int_{\tau_0}^{\tau_{end}} d\tau \epsilon^2 a^2 \xi_1(\tau) \xi_2(\tau) \xi_3(\tau) + \mathcal{O}(\epsilon^3) \right] \quad (3.27)$$

$$I_{\epsilon\eta'} \propto \Re \left[ \prod_i u_i(\tau_{end}) \int_{\tau_0}^{\tau_{end}} d\tau \epsilon \eta' a^2 \xi_1(\tau) \xi_2(\tau) \xi_3(\tau) \right] \quad (3.28)$$

where  $\xi_n$  is either  $u_{k_n}^*$  or  $du_{k_n}^*/d\tau$ . In a single field model  $u_k(\tau) \rightarrow \text{const}$  after Hubble crossing as it freezes out, while  $u_k(\tau) \rightarrow e^{-ik\tau}$  oscillates rapidly at early times, so its contribution to the integral tends to cancel. Thus the integral is dominated by the range of  $\tau$  during which the modes leave the horizon.

Now let us consider the potential (2.5). We expect  $\epsilon \ll 1$ , since while the step in the potential is steep, it is very small. This makes (3.27) negligible. However,  $\eta$  and  $\eta'$  can clearly be very large as the  $H$  changes rapidly over a very short time. This flagrant violation of slow roll means that we expect a large contribution from the  $I_{\epsilon\eta'}$  term in the integral, of the order  $\Delta\tau\eta'/\epsilon \times I_{\epsilon^2}$ , where  $\Delta\tau$  is the acceleration time for the inflaton by the feature. From the qualitative estimation in Sec. 2, we know this is  $18c^{3/2}/(\sqrt{6}d\epsilon^2) \times I_{\epsilon^2}$ . The best parameters from Covi *et al.* for a step that matches the low- $\ell$  glitch seen in current CMB data are  $c = 0.0018$  and  $d = 0.022$  [11]. Thus we expect a boost in the 3-point statistic of  $\mathcal{O}(100 \sim 1000)$  at scales affected by the step. Factoring in the baseline value of the estimator for the 3-point function being proportional to  $\epsilon$ , we see that this pushes the expected value up to  $\mathcal{O}(10)$  from  $\mathcal{O}(10^{-2})$ .

We now focus on the  $I_{\epsilon\eta'}$  term, and relegate the discussion of the rest of the subleading contribution to an appendix (where a field redefinition term is also subleading since the effect of the feature dies away towards the boundary). So our leading term is

$$i \left( \prod_i u_i(\tau_{end}) \right) \int_{-\infty}^{\tau_{end}} d\tau a^2 \epsilon \eta' \left( u_1^*(\tau) u_2^*(\tau) \frac{d}{d\tau} u_3^*(\tau) + \text{two perm} \right) (2\pi)^3 \delta^3 \left( \sum_i \mathbf{k}_i \right) + \text{c.c.} , \quad (3.29)$$

where the “two perm” stands for two other terms that are symmetric under permutations of the indices 1, 2 and 3. (1, 2, 3 stand for  $k_1, k_2, k_3$ , respectively.)

Thus task of the numerical calculation is to solve the equations of motion to get  $u_k(\tau)$ , and then evaluate the solutions in (3.29) and integrate. The contributions from the other five terms in the interaction Hamiltonian (3.17) in the appendix can be calculated in a similar fashion to (3.29).

## 4 Numerical Method

Our goal is to integrate the 3-point correlation functions, which are products of the perturbation mode and background functions. Thus we first need to solve the equations of motions for the fields, and then plug them into the integrals described in Sec. 3. The equations of motion for the background fields and the perturbations are

$$H(\tau) = \frac{a'}{a^2}, \quad (4.30)$$

$$\frac{d^2 a}{d\tau^2} = \frac{a}{6M_p^2} (-\phi'^2 + 4a^2 V(\phi)), \quad (4.31)$$

$$\frac{d^2 \phi}{d\tau^2} = -2\frac{a'}{a}\phi' - a^2 \frac{dV}{d\phi}, \quad (4.32)$$

$$\frac{d^2 v_k}{d\tau^2} = -\left(k^2 - \frac{z''}{z}\right)v_k, \quad (4.33)$$

where  $\tau$  is our time parameter. We choose initial conditions and units for  $\tau$  such that the step occurs around  $\tau = -1$ , and the mode with comoving wavenumber  $k = 1$  crosses the horizon at the same point. The initial conditions of the perturbations are given by (3.26).

The next step is to integrate the 3-point correlation function itself, i.e. equations (3.29) and equations (A.48) to (A.50). They all have the form (3.27) and (3.28). At early times the integrand is highly oscillatory and the net contribution per period is thus very small. However the early time limit of the integral must be handled with care, since a sharp cutoff imposed by a finite initial time will introduce a spurious contribution of  $\mathcal{O}(1)$  into the result.

Analytically, the standard procedure is to Wick rotate the integral slightly into the imaginary plane [6, 21, 22] in order to eliminate the oscillatory terms. Unfortunately, it is not straightforward to implement this approach numerically. Instead we use a trick by introducing a “damping” factor  $\beta$  into the integrand

$$I_{e^2} \propto \int_{\tau_0}^{\tau_{end}} d\tau a^2 \epsilon^2 \xi_1 \xi_2 \xi_3 \times e^{\beta(k_1+k_2+k_3)(\tau-\tau_{end})}, \quad (4.34)$$

and similarly for the  $I_{\eta'\epsilon}$  term. This is approximately equivalent to rotating the contour integral from the real axis slightly into the imaginary plane  $\tau \rightarrow \tau(1 - i\beta)$ . The error introduced by this numerical procedure can be estimated by taking the difference between the integration over  $e^{i(k_1+k_2+k_3)\tau}$  and  $e^{(i+\beta)(k_1+k_2+k_3)\tau}$ . The relative error is thus  $\beta$ . If we choose  $\beta$  such that

$$|\beta k \tau_{crossing}| \ll 1, \quad (4.35)$$

$$|\beta k \tau_{early}| \gg 1, \quad (4.36)$$

then this contribution is negligible, recalling that  $\tau < 0$ .

Given the choice of initial conditions, we chose  $\beta = 0.05$  in our code. This choice damps out the oscillation contributions at early times and thus renders the choice of initial conditions irrelevant, while having no effect on the integrand during Hubble crossing, which

provides the dominant contribution to the 3-point function. We tested this scheme against the known analytical results for 3-point functions, which we match to within a few percent. However, the value of  $\beta$  needs to be set by hand in our code, and while this approach is suitable for an initial survey, we plan to adopt a more elegant scheme in the future. As an aside, the imaginary component of the integral goes to infinity, scaling as  $a^2$ . However, as long as we stop the integration a few e-folds after horizon crossing, the integration is stable.

## 5 Results and Discussion

### 5.1 Shape and Scale

Every 3-point correlation function has two main attributes: shape and scale. Unlike previous treatments, we cannot assume that the 3-point function is scale invariant. Before we compare the analytical and the numerical results, let us define a more useful parameter than the rather unwieldy raw 3-point function. We will begin with a general form of the 3-point,

$$\langle \zeta(\mathbf{k}_1)\zeta(\mathbf{k}_2)\zeta(\mathbf{k}_3) \rangle = (2\pi)^7 N \delta^3(\mathbf{k}_1 + \mathbf{k}_2 + \mathbf{k}_3) \frac{1}{\prod_i k_i^3} \mathcal{G}(\mathbf{k}_1, \mathbf{k}_2, \mathbf{k}_3). \quad (5.37)$$

We have factored out the product  $1/\prod_i k_i^3$  by appealing to the fact the mode function  $u(\tau) \sim k^{-3/2} \exp(-ik\tau)$  during inflation and there are 6 factors of  $u$  in the 3-point function. The function  $\mathcal{G}$  depends on the details of the integrals listed in Sect. 3 and  $N$  is some constant that we will come back to later. If the slow roll parameters stay small and constant, it can be shown [6, 21, 22] that we can factor the power spectrum out of  $\mathcal{G}$

$$\langle \zeta(\mathbf{k}_1)\zeta(\mathbf{k}_2)\zeta(\mathbf{k}_3) \rangle = (2\pi)^7 \delta^3(\mathbf{k}_1 + \mathbf{k}_2 + \mathbf{k}_3) (P_k^\zeta)^2 \frac{1}{\prod_i k_i^3} \mathcal{A}(\mathbf{k}_1, \mathbf{k}_2, \mathbf{k}_3), \quad (5.38)$$

where  $\mathcal{A}$  is a quantity of  $\mathcal{O}(k^3)$  and the convention here follows Ref. [22]. In terms of  $\mathcal{G}$ ,

$$N\mathcal{G} = (P_k^\zeta)^2 \mathcal{A}. \quad (5.39)$$

Since the power spectrum is statistically isotropic [36], we assume that this is also true in the bispectrum and thus we will impose rotational symmetry so that, combined with the conserved momentum constraint, the 3-point correlation function only depends on the amplitudes of the  $k$ 's.

Recall the definition of  $f_{NL}$ , equation (1.1), which is often used when computing the amount of non-Gaussianities in the CMB sky [37, 38, 1, 8]. Current constraints on  $f_{NL}$ , from 3 years of WMAP data are [39]

$$-36 < f_{NL} < 100. \quad (5.40)$$

However, as pointed out in [30], this ansatz assumes that the 3-point correlation function has the following *local* form

$$\langle \zeta(\mathbf{k}_1)\zeta(\mathbf{k}_2)\zeta(\mathbf{k}_3) \rangle_{local} = (2\pi)^7 \delta^3(\mathbf{k}_1 + \mathbf{k}_2 + \mathbf{k}_3) \left( -\frac{3}{10} f_{NL} (P_k^\zeta)^2 \right) \frac{\sum_i k_i^3}{\prod_i k_i^3}, \quad (5.41)$$

or, in terms of  $\mathcal{A}$

$$\mathcal{A}_{local} = -\frac{3}{10}f_{NL}\Sigma_i k_i^3. \quad (5.42)$$

In other words, the constraint (5.40) is applicable only if the primordial non-Gaussianities have the local form (5.41).

Since equation (1.1) does not contain an explicit scale, this form is scale-invariant (neglecting the  $\mathcal{O}(\epsilon)$  correction terms)

$$\langle \zeta(\mathbf{k}_1)\zeta(\mathbf{k}_2)\zeta(\mathbf{k}_3) \rangle_{local} = \lambda^9 \langle \zeta(\lambda\mathbf{k}_1)\zeta(\lambda\mathbf{k}_2)\zeta(\lambda\mathbf{k}_3) \rangle_{local}. \quad (5.43)$$

Note that there is a small violation of scale-invariance in the 3-point correlation function stemming from the power spectrum term which we have ignored in the proceeding argument. In fact, equation (5.41) itself hides a further ambiguity: at what value of  $k$  are we evaluating the power spectrum? This omission is justified if we assume that the power spectrum is almost scale-invariant, which is true for most “standard” slow roll single scalar field models. However, for the step potential we are considering, the power spectrum itself undergoes drastic oscillations of  $\mathcal{O}(1)$ . We will come back to this point later.

## 5.2 Quadratic ( $m^2\phi^2$ ) inflation

As a warm up exercise, we reproduce the results of a simple slow roll inflation model, for which we have an analytical result for the 3-point function [6]. We work with standard quadratic chaotic inflation model with the potential

$$V(\phi) = \frac{1}{2}m^2\phi^2 \quad (5.44)$$

where  $m = 10^{-6}M_p$ .

Following [6], we can write down the explicit form of  $\mathcal{A}$

$$\mathcal{A}_{SR} = \epsilon \left( -\frac{1}{8}\Sigma_i k_i^3 + \frac{1}{8}\Sigma_{i \neq j} k_i k_j^2 + \frac{1}{k_1 + k_2 + k_3} \Sigma_{i > j} k_i^2 k_j^2 \right) + \eta \left( \frac{1}{8}\Sigma_i k_i^3 \right) + \mathcal{O}(\epsilon^2), \quad (5.45)$$

where  $\mathcal{O}(\epsilon^2)$  terms include  $\eta'$ . Comparing this to the local form equation (5.42) we can see that for the equilateral case,  $-3f_{NL}/10 = 11\epsilon/8 + 3\eta/4 = 17\epsilon/8$  where the second equality comes from the fact that  $\eta = 2\epsilon$  for the potential (5.44). In the other extreme of the squeezed triangle case,  $-3f_{NL}/10 = 2\epsilon + \eta = 4\epsilon$ . This result was first derived by Maldacena, who pointed out that for single field slow roll inflationary models,  $f_{NL} = \mathcal{O}(\epsilon)$  and is thus unobservable. We compared our code’s results to equation (5.45), and as Figure 2 shows, our code is accurate to within a few percent, which is within the error expected from the analytical estimate itself.

Since the potential has no feature in it, the 3-point correlation function is essentially “scale independent”. However, this does not imply that all triangles have identical 3-point functions – and the computed values can and does depend on the shape of the momentum triangle, as illustrated by Fig. 3. Rather, scale invariance tells us that, if we scale  $k_1$ ,  $k_2$  and  $k_3$  by the same factor, the 3-point function is effectively unchanged.

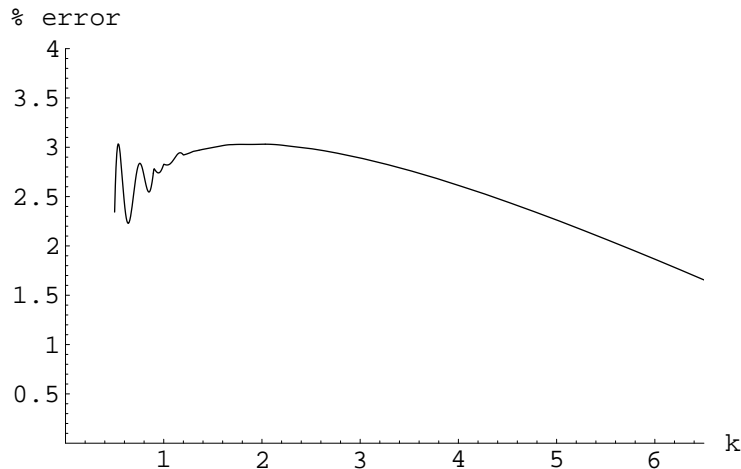


Figure 2: Comparison of  $\mathcal{A}/k^3$  between the analytical slow roll results of equation (5.45) and numerical results from our code, for the equilateral case where  $k_1 = k_2 = k_3 = k$  run from  $0.5 < k < 6.5$ . The plot shows the discrepancy between the two sets of values. The rapid oscillation at small  $k$  is numerical noise. Since the  $k$  space spans a few efolds, we have included the contribution from the  $\epsilon$  running when computing the analytic estimate but ignored the  $\mathcal{O}(\epsilon^2)$  terms. As we can see, the two results agree to within a few percent.

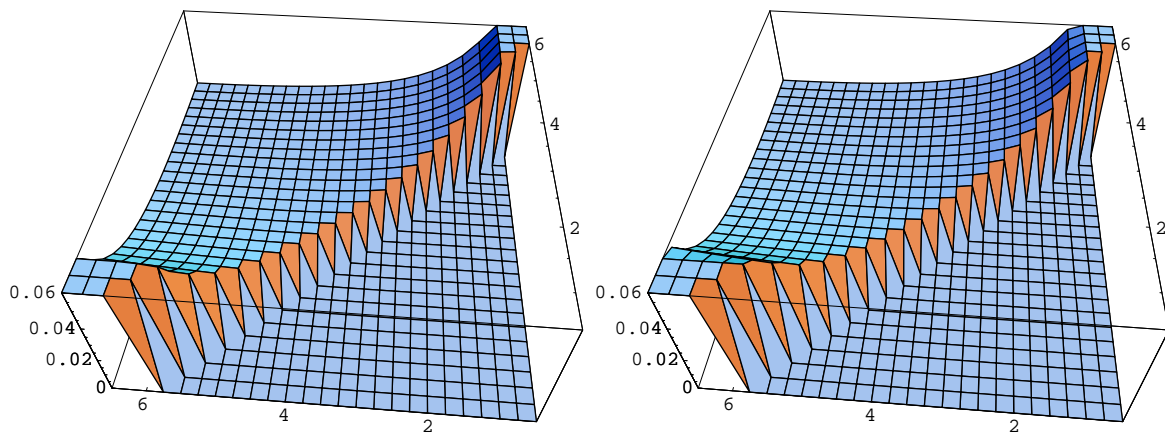


Figure 3: A comparison of the analytically calculated (left) and numerically generated (right)  $\mathcal{A}/(k_1 k_2 k_3)$  results for the  $m^2 \phi^2$  model. The analytical results are computed using (5.45), ignoring the  $\mathcal{O}(\epsilon^2)$  terms and the numerical results are generated using our code neglecting the same terms. The  $k$ -space spans  $k_1, k_2$  from 0.5 to 6.5 with the two plots fixed at  $k_3 = 6.5$  and the triangle inequality conditions  $k_i \leq k_j + k_l, i \neq j, l$  imposed. By eye, the two results are almost indistinguishable.

### 5.3 Step potential

Confident that our code is robust, we now compute the 3-point correlation functions for the step potential (2.5). We focus on the best fit model of Covi *et al.* [11] for a step which affects modes at large angular scales, namely where  $(c, \phi_s, d) = (0.0018, 14.81M_p, 0.022)$ . We choose the same inflaton mass  $m = 10^{-6}M_p$  used with the  $m^2\phi^2$  model, so that we can compare the results.

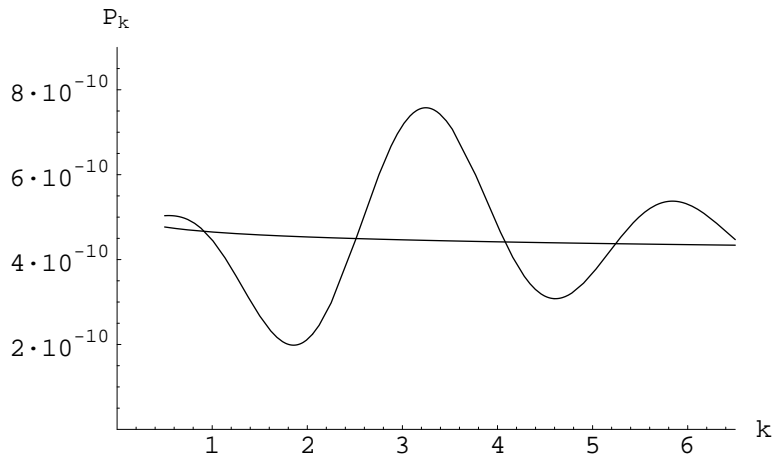


Figure 4: The power spectrum for the standard  $m^2\phi^2$  model and the step potential (2.5) for a decade of  $k$ . The power spectrum for the latter demonstrates a characteristic ringing; this behavior has been suggested by [11] as a possible explanation for the existence of outliers in the WMAP 3 year data.

Consider the power spectrum, Figure (4). As first described in [20], the violation of slow roll induces a temporary growing/decaying behavior in the evolution of the modes before horizon crossing, resulting in a “ringing” of the power spectrum. Thus we cannot simply factor out the power spectrum from  $\mathcal{G}$  as we have done in equation (5.38); doing so will introduce spurious contributions to any statistic that we might obtain. On the other hand, we expect the 3-point correlation to be of order  $(P_k^\zeta)^2$ , so if we set  $N = \tilde{P}_k^2$  in equation (5.37) where  $\tilde{P}_k \equiv 4 \times 10^{-10}$  (i.e. the observed value of the power spectrum), then the dimensionless quantity

$$\frac{\mathcal{G}(k_1, k_2, k_3)}{k_1 k_2 k_3} = \frac{1}{\delta^3(\mathbf{k}_1 + \mathbf{k}_2 + \mathbf{k}_3)} \frac{(k_1 k_2 k_3)^2}{\tilde{P}^2 (2\pi)^7} \langle \zeta(\mathbf{k}_1) \zeta(\mathbf{k}_2) \zeta(\mathbf{k}_3) \rangle \quad (5.46)$$

is what we want to plot. This quantity has the great advantage that the strong  $k^9$  running from the scaling of the 3-point correlation function (see for example equation (5.43)) is factored out, so we are left with the scaling that are purely generated from the non-linear evolution of the modes themselves.

Consider the equilateral case, Figure (5). Similar to the power spectrum, the presence of the step induces a ringing of the equilateral bispectrum. The ringing frequency in the 3-point function is roughly 1.5 times that in power spectrum – which is understood as being due to the presence of three factors of  $\zeta$  in the integrand instead of two.

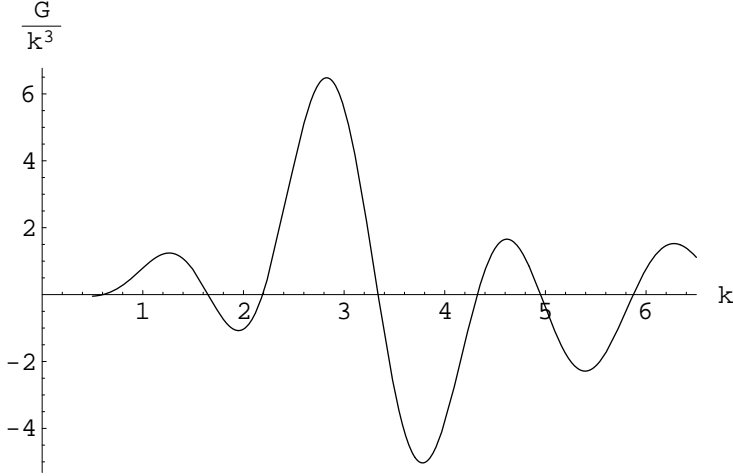


Figure 5: The running of non-Gaussianity  $\mathcal{G}/k_1k_2k_3$  (in the equilateral case  $k_1 = k_2 = k_3 \equiv k$ ) for the large scale step potential model of  $(c, \phi_s, d) = (0.0018, 14.81M_p, 0.022)$ . For comparison, the standard slow roll model will yield  $\mathcal{G}/k_1k_2k_3 \approx \mathcal{O}(\epsilon)$ .

The plots in Figures 6 illustrate the complicated landscape of the non-Gaussianities. Compared to the  $\mathcal{O}(\epsilon)$  amplitude of the  $m^2\phi^2$  model, the non-Gaussianities here are magnified several hundreds fold and may even be larger for other parameters of the step potential which are still viable (Figure 8). As we explained in section (3), the dominant contribution to the non-Gaussianities comes from the  $\eta'$  term (Figure (1)). We estimated there that the boost in non-Gaussianities will be of order  $18c^{3/2}/(\sqrt{6}d\epsilon)$  and our numerical results confirm our suspicions; this scaling remains consistent when we vary the parameter space (Figure (8)).

In Figure 7, we plot the integrand  $(k_1k_2k_3)^2I_{\eta'\epsilon}$  with respect to  $\tau$  for the modes which cross the Hubble horizon around the step. We have suppressed the early time oscillations via the damping trick we mentioned before in order to tease out the actual contribution to the integral. The step also occurs around this time. Comparing this with the  $\eta'$  plot Figure (1), we see that the oscillatory nature of  $u_1^*u_2^*u_3^*$  modulates the single hump of  $\eta'$ , yielding complicated structures. Depending on the combined phases of the modes, the modulation can be both constructive and destructive, leading to the “ringing” of the primordial bispectrum. The non-linear interactions between the modes have become dominant due to the large coupling term  $\epsilon\eta'$  around crossing, mixing up the perturbations in non-trivial manner and generating large departures from Gaussianity. This is in contrast the ringing of the power spectrum which is caused by the change in the effective mass of the modes as they cross the horizon.

To bound this specific non-Gaussian signal with current WMAP data, we would have to redo the full sky analysis using the data for our complicated scale and shape dependent predictions of the bispectrum. This is not a trivial task and requires new methods to be developed before we can approach the problem. A brute force computation of the likelihood is computationally daunting since the bispectrum here is clearly unfactorizable into a products of separate integrals over the  $k$ 's.

However, we can make some guesses. We have previously alluded to the fact that the

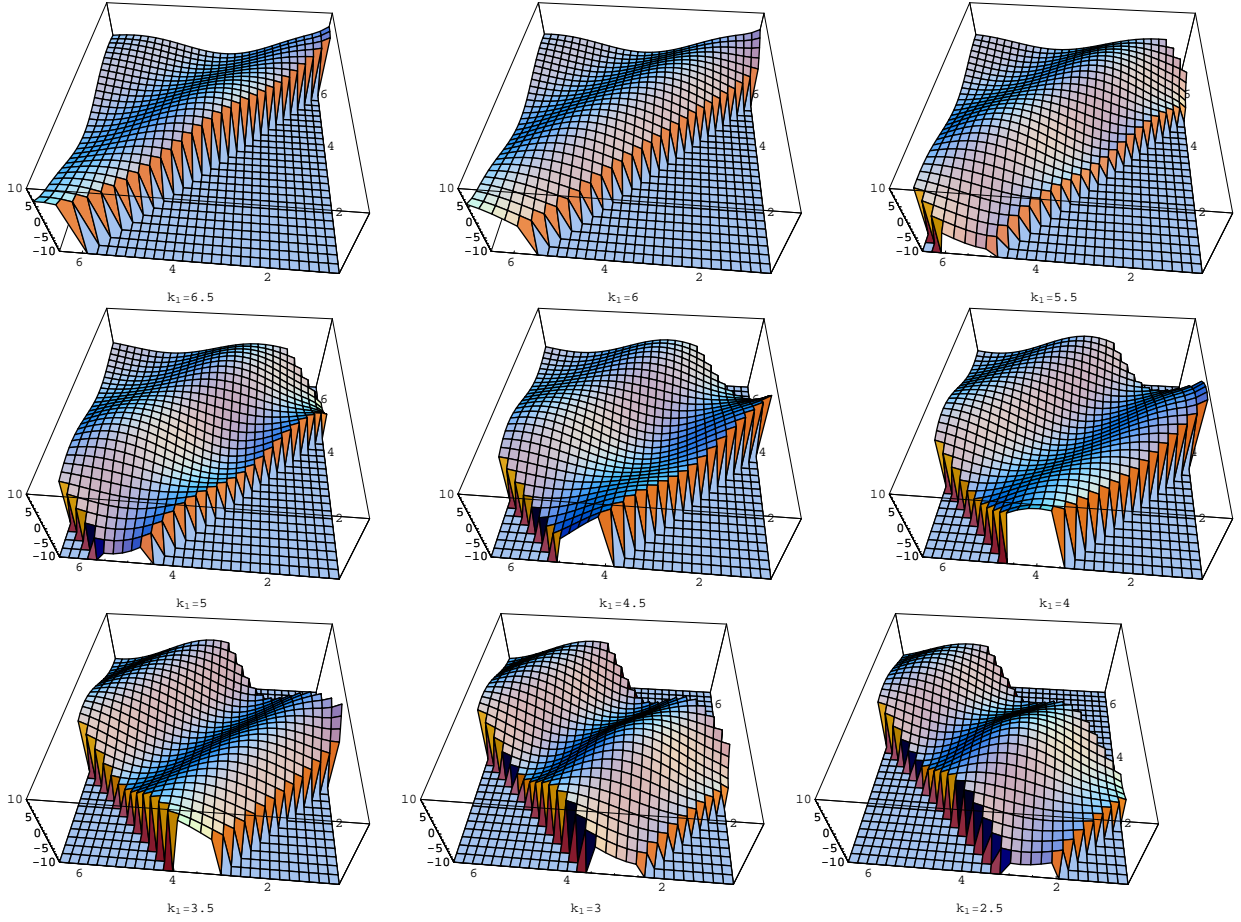


Figure 6: The shape of non-Gaussianities  $\mathcal{G}/k_1k_2k_3$  for the large scale step potential model of  $(c, \phi_s, d) = (0.0018, 14.81M_p, 0.022)$ , with  $k_1$  ranging from 6.5 to 2.5 going from top left to bottom right. We have set the forbidden triangle regions outside of  $k_i \leq k_j + k_l$ ,  $i \neq j, l$  to  $-10$  for visualization purposes.

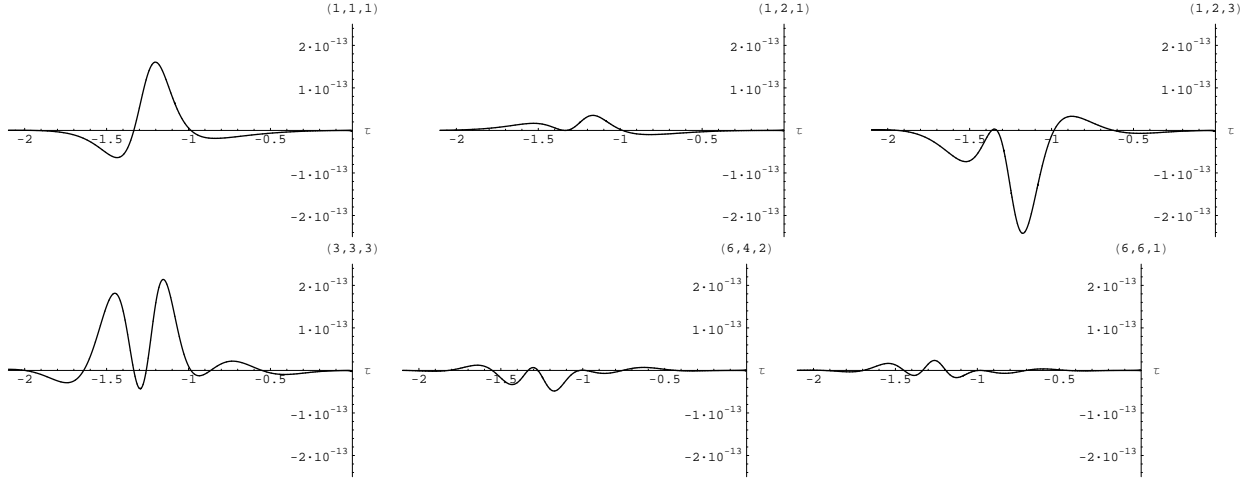


Figure 7: The real component of the integrand  $(k_1 k_2 k_3)^2 a^2 \epsilon \eta' u_1(0) u_2(0) u_3(0) u_1^* u_2^* u_3^*$  plotted for the modes  $(k_1, k_2, k_3)$ , with the step occurring around  $\tau = -1$  and inflation ending at  $\tau = 0$ .

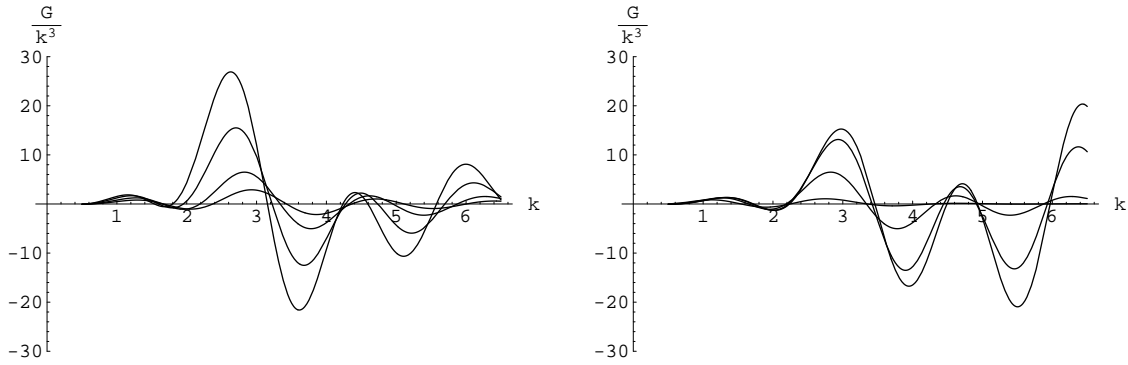


Figure 8: Variation of  $\mathcal{G}/k^3$  in response to changing the parameters of the step for the equilateral triangle case. The left (right) plot describes the variation of  $c$  ( $d$ ) from the smallest to biggest amplitude in the order  $c = 0.0009, 0.0018, 0.0036, 0.0054$  fixing  $d = 0.022$  ( $d = 0.044, 0.022, 0.011, 0.0074$  fixing  $c = 0.0018$ ). We keep the location of the step fixed at  $\phi_s = 14.81 M_p$ .

statistic (5.46) is similar to  $f_{NL}$ . By comparing equation (5.42) to equation (5.46), we see that roughly

$$f_{NL} \sim -\frac{10k_1k_2k_3}{3\Sigma_i k_i^3} \frac{\mathcal{G}(k_1, k_2, k_3)}{k_1k_2k_3}. \quad (5.47)$$

Since the factor  $10k_1k_2k_3/3\Sigma_i k_i^3$  is roughly of  $\mathcal{O}(1)$  then  $f_{NL} \sim \mathcal{G}(k_1, k_2, k_3)/k_1k_2k_3 \sim \mathcal{O}(10)$  which is within sights of the next generation CMB experiments [8]. However, in our case only a subset of all possible triangles we could draw on the sky have a large 3-point function, which increases the risk that cosmic variance will swamp any signal. On the other hand, since we have a specific template for the 3-point function, which can then be cross-correlated with the 2-point function associated with any putative step, we can put tighter constraints on the 3-point function for the step potential than would be possible if we did not know the form of  $\mathcal{G}$ .

## 6 Conclusion

While simple models of slow roll inflation do not exhibit observable non-Gaussianities, the space of models of inflation that can produce a power spectrum which fits the CMB data is infinite. To discriminate between these degenerate models, some other independent statistic derived from the CMB must be used and the bispectrum is becoming the most promising candidate for this role.

Unlike the power spectrum, the computation of the bispectrum for a given inflationary models is a messy affair, tractable only in the simplest models as we have to follow the entire history of non-linear interaction for all the modes. In this paper, we have developed a robust numerical code which can compute the 3-point correlation function for a non-slow roll single field model.

Using this method, we numerically integrated the 3-point correlation functions for a class of inflationary models where slow roll is violated for a brief moment. We show that the addition of this step breaks the scale invariance of the bispectrum in a non-trivial way, leading to large non-Gaussianities. This numerical technique can be extended to solve more complicated problems such as multifield models of inflation [40, 41] and to compute higher statistics such as the trispectrum [16].

Mirroring the behavior of the power spectrum, a temporary violation of slow roll introduces a ringing into the bispectrum, resulting in a structure much like the transient vibrations of a rug being beaten. These large non-Gaussianities are generated when the non-linear coupling between the modes,  $\epsilon\eta'$ , becomes temporarily large during this period of non-slow roll behavior. In order to check whether we can constrain such models with data, a full sky analysis must be undertaken with either current or future data, a task which is beyond the scope of this paper. However, we argue that at least for the models considered in this paper, the non-Gaussianities may be large enough to be within reach of the Planck satellite.

In the near future we can expect even better quality data of the CMB to become available, opening up the possibility of doing cross correlation of higher order statistics such as the bispectrum with the power spectrum. Such correlations provide to with a powerful

consistency check on any models of inflation where a sharp feature is added to the potential in order to improve the fit to the 2-point function of power spectrum. Consequently, we have laid the groundwork for a constructing an analog of the “consistency relationship” that applies to simple models of slow roll inflation, where the amplitude and slope of the scalar and tensor spectra are expressed as functions of just three independent parameters - the observed amplitude of the scalar spectrum, and the first two slow roll parameters,  $\epsilon$  and  $\eta$ . In this case considered here, the parameters that describe any step or other near-discontinuity would fix both the 2- and 3-point functions, yielding a consistency test for a very broad class of inflationary models. In practice we could fit separately to the 2- and 3-point functions and then check that the results were in accord with our chosen potential. Alternatively, one could simultaneously include information from both the power spectrum and bispectrum into the cosmological parameter estimation process. In this case, we could fit directly to the parameters  $c$ ,  $d$  and  $\phi_s$  (along with the “average” slow roll parameters), generalizing the approach of [42, 43]. Finally, if it ever becomes possible to determine the 3-point function from observations of large scale structure, this information would further tighten the constraints on models where slow roll is briefly violated.

## Acknowledgments

We thank Wayne Hu, Eiichiro Komatsu, Hiranya Peiris, Kendrick Smith and Henry Tye for a number of useful discussions. XC thanks the physics department of Yale university and KITP for their hospitality. XC is supported in part by the National Science Foundation under grant PHY-035505. RE and EAL are supported in part by the United States Department of Energy, grant DE-FG02-92ER-40704.

## A Other terms

In Section 3, we have given the expressions for the leading non-Gaussianity in the case when  $\eta$  is large but  $\epsilon$  remains small. In this appendix, we give the expressions for the subleading terms for this case from the Hamiltonian (3.17).

The subleading contributions come from the first line of (3.17). Contribution from  $a^3\epsilon^2\zeta\dot{\zeta}^2$  term:

$$2i \int_{-\infty}^{\tau_{end}} d\tau a^2\epsilon^2 \left( \prod_i u_i(\tau_{end}) \right) \left( u_1^* \frac{du_2^*}{d\tau} \frac{du_3^*}{d\tau} + \text{two perm} \right) (2\pi)^3 \delta^3(\sum_i \mathbf{k}_i) + \text{c.c.} . \quad (\text{A.48})$$

Contribution from  $a\epsilon^2\zeta(\partial\zeta)^2$  term:

$$-2i \int_{-\infty}^{\tau_{end}} d\tau a^2\epsilon^2 \left( \prod_i u_i(\tau_{end}) u_i^*(\tau) \right) (\mathbf{k}_1 \cdot \mathbf{k}_2 + \text{two perm}) (2\pi)^3 \delta^3(\sum_i \mathbf{k}_i) + \text{c.c.} . \quad (\text{A.49})$$

Contribution from  $-2a\epsilon\dot{\zeta}(\partial\zeta)(\partial\chi)$  term:

$$-2i \int_{-\infty}^{\tau_{end}} d\tau a^2 \epsilon^2 \left( \prod_i u_i(\tau_{end}) \right) \left( u_1^* \frac{du_2^*}{d\tau} \frac{du_3^*}{d\tau} \frac{\mathbf{k}_1 \cdot \mathbf{k}_2}{k_2^2} + \text{five perm} \right) (2\pi)^3 \delta^3 \left( \sum_i \mathbf{k}_i \right) + \text{c.c.} . \quad (\text{A.50})$$

The redefinition (3.15) contributes

$$\frac{\eta}{2} |u_2|^2 |u_3|^2 \Big|_{\tau \rightarrow \tau_{end}} (2\pi)^3 \delta^3 \left( \sum_i \mathbf{k}_i \right) + \text{two perm} . \quad (\text{A.51})$$

Note that in Ref. [6, 21, 22], where sharp features are absent, these four terms give leading contributions to non-Gaussianities.

The last two terms in (3.17) are further suppressed by  $\epsilon$ , but for completeness we list their contribution in the following. Contribution from  $(\epsilon/2a)\partial\zeta\partial\chi\partial^2\chi$  term:

$$\frac{i}{2} \int_{-\infty}^{\tau_{end}} d\tau a^2 \epsilon^3 \left( \prod_i u_i(\tau_{end}) \right) \left( u_1^* \frac{du_2^*}{d\tau} \frac{du_3^*}{d\tau} \frac{\mathbf{k}_1 \cdot \mathbf{k}_2}{k_2^2} + \text{five perm} \right) (2\pi)^3 \delta^3 \left( \sum_i \mathbf{k}_i \right) + \text{c.c.} . \quad (\text{A.52})$$

Contribution from  $(\epsilon/4a)(\partial^2\zeta)(\partial\chi)^2$  term:

$$\frac{i}{2} \int_{-\infty}^{\tau_{end}} d\tau a^2 \epsilon^3 \left( \prod_i u_i(\tau_{end}) \right) \left( u_1^* \frac{du_2^*}{d\tau} \frac{du_3^*}{d\tau} k_1^2 \frac{\mathbf{k}_2 \cdot \mathbf{k}_3}{k_2^2 k_3^2} + \text{two perm} \right) (2\pi)^3 \delta^3 \left( \sum_i \mathbf{k}_i \right) + \text{c.c.} . \quad (\text{A.53})$$

## References

- [1] D. N. Spergel *et al.*, “Wilkinson Microwave Anisotropy Probe (WMAP) three year results: Implications for cosmology,” arXiv:astro-ph/0603449.
- [2] R. Scoccimarro, E. Sefusatti and M. Zaldarriaga, Phys. Rev. D **69**, 103513 (2004) [arXiv:astro-ph/0312286].
- [3] M. Liguori, F. K. Hansen, E. Komatsu, S. Matarrese and A. Riotto, Phys. Rev. D **73** (2006) 043505 [arXiv:astro-ph/0509098].
- [4] T. Pyne and S. M. Carroll, “Higher-Order Gravitational Perturbations of the Cosmic Microwave Phys. Rev. D **53**, 2920 (1996) [arXiv:astro-ph/9510041].
- [5] E. Komatsu and D. N. Spergel, Phys. Rev. D **63**, 063002 (2001) [arXiv:astro-ph/0005036].
- [6] J. M. Maldacena, JHEP **0305**, 013 (2003) [arXiv:astro-ph/0210603].
- [7] L. Verde, L. M. Wang, A. Heavens and M. Kamionkowski, Mon. Not. Roy. Astron. Soc. **313**, L141 (2000) [arXiv:astro-ph/9906301].
- [8] C. Hikage, E. Komatsu and T. Matsubara, “Primordial Non-Gaussianity and Analytical Formula for Minkowski Functionals arXiv:astro-ph/0607284.
- [9] K. M. Smith and M. Zaldarriaga, arXiv:astro-ph/0612571.
- [10] H. V. Peiris *et al.*, “First year Wilkinson Microwave Anisotropy Probe (WMAP) observations: Astrophys. J. Suppl. **148**, 213 (2003) [arXiv:astro-ph/0302225].
- [11] L. Covi, J. Hamann, A. Melchiorri, A. Slosar and I. Sorbera, arXiv:astro-ph/0606452.
- [12] T. Okamoto and W. Hu, Phys. Rev. D **66**, 063008 (2002) [arXiv:astro-ph/0206155].
- [13] N. Kogo and E. Komatsu, Phys. Rev. D **73**, 083007 (2006) [arXiv:astro-ph/0602099].
- [14] C. T. Byrnes, M. Sasaki and D. Wands, arXiv:astro-ph/0611075.
- [15] D. Seery and J. E. Lidsey, arXiv:astro-ph/0611034.
- [16] D. Seery, J. E. Lidsey and M. S. Sloth, arXiv:astro-ph/0610210.
- [17] W. Hu, Phys. Rev. D **64**, 083005 (2001) [arXiv:astro-ph/0105117].
- [18] M. x. Huang and G. Shiu, arXiv:hep-th/0610235.
- [19] E. Komatsu *et al.*, Astrophys. J. Suppl. **148**, 119 (2003) [arXiv:astro-ph/0302223].
- [20] J. A. Adams, B. Cresswell and R. Easther, Phys. Rev. D **64**, 123514 (2001) [arXiv:astro-ph/0102236].

- [21] D. Seery and J. E. Lidsey, *JCAP* **0506**, 003 (2005) [arXiv:astro-ph/0503692].
- [22] X. Chen, M. x. Huang, S. Kachru and G. Shiu, arXiv:hep-th/0605045.
- [23] X. Chen, *Phys. Rev. D* **72**, 123518 (2005) [arXiv:astro-ph/0507053].
- [24] E. Silverstein and D. Tong, *Phys. Rev. D* **70**, 103505 (2004) [arXiv:hep-th/0310221].
- [25] X. Chen, *Phys. Rev. D* **71**, 063506 (2005) [arXiv:hep-th/0408084].
- [26] C. Armendariz-Picon, T. Damour and V. F. Mukhanov, *Phys. Lett. B* **458**, 209 (1999) [arXiv:hep-th/9904075].
- [27] M. Alishahiha, E. Silverstein and D. Tong, *Phys. Rev. D* **70**, 123505 (2004) [arXiv:hep-th/0404084].
- [28] S. E. Shandera and S. H. Tye, *JCAP* **0605**, 007 (2006) [arXiv:hep-th/0601099].
- [29] S. Kecskemeti, J. Maiden, G. Shiu and B. Underwood, *JHEP* **0609**, 076 (2006) [arXiv:hep-th/0605189].
- [30] D. Babich, P. Creminelli and M. Zaldarriaga, *JCAP* **0408**, 009 (2004) [arXiv:astro-ph/0405356].
- [31] A. A. Starobinsky, *JETP Lett.* **55**, 489 (1992) [*Pisma Zh. Eksp. Teor. Fiz.* **55**, 477 (1992)].
- [32] R. Arnowitt, S. Deser and C. W. Misner, *Phys. Rev.* **117** (1960) 1595.
- [33] V. F. Mukhanov, H. A. Feldman and R. H. Brandenberger, “Theory of cosmological perturbations. Part 1. Classical perturbations. Part 2. Quantum theory of perturbations. Part 3. Extensions,” *Phys. Rept.* **215**, 203 (1992).
- [34] A. Gangui, F. Lucchin, S. Matarrese and S. Mollerach, *Astrophys. J.* **430**, 447 (1994) [arXiv:astro-ph/9312033].
- [35] V. Acquaviva, N. Bartolo, S. Matarrese and A. Riotto, *Nucl. Phys. B* **667**, 119 (2003) [arXiv:astro-ph/0209156].
- [36] A. Hajian and T. Souradeep, *Astrophys. J.* **597**, L5 (2003) [arXiv:astro-ph/0308001].
- [37] E. Komatsu, arXiv:astro-ph/0206039.
- [38] E. Komatsu, D. N. Spergel and B. D. Wandelt, “Measuring primordial non-Gaussianity in the cosmic microwave background,” *Astrophys. J.* **634**, 14 (2005) [arXiv:astro-ph/0305189].
- [39] P. Creminelli, L. Senatore, M. Zaldarriaga and M. Tegmark, arXiv:astro-ph/0610600.
- [40] T. Battefeld and R. Easther, arXiv:astro-ph/0610296.

- [41] F. Vernizzi and D. Wands, JCAP **0605**, 019 (2006) [arXiv:astro-ph/0603799].
- [42] H. Peiris and R. Easther, JCAP **0610**, 017 (2006) [arXiv:astro-ph/0609003].
- [43] H. Peiris and R. Easther, JCAP **0607**, 002 (2006) [arXiv:astro-ph/0603587].
- [44] J. A. Adams, G. G. Ross and S. Sarkar, Nucl. Phys. B **503**, 405 (1997) [arXiv:hep-ph/9704286].